THE JOURNAL OF PHYSICAL CHEMISTRY B

ARTICLE

pubs.acs.org/JPCB

Bovine Insulin–Phosphatidylcholine Mixed Langmuir Monolayers: Behavior at the Air–Water Interface

S. Pérez-López, N.M. Blanco-Vila, and N. Vila-Romeu*

Department of Physical Chemistry-Faculty of Sciences in Ourense, University of Vigo; Campus As Lagoas s/n 32004 Ourense, Spain

ABSTRACT: The behavior of the binary mixed Langmuir monolayers of bovine insulin (INS) and phosphatidylcholine (PC) spread at the air–water interface was investigated under various subphase conditions. Pure and mixed monolayers were spread on water, on NaOH and phosphate-buffered solutions of pH 7.4, and on Zn^{2+}-containing solutions. Miscibility and interactions between the components were studied on the basis of the analysis of the surface pressure (π)–mean molecular area (A) isotherms, surface compression modulus (C_s^{-1})–π curves, and plots of A versus mole fraction of INS (X_{INS}). Our results indicate that intermolecular interactions between INS and PC depend on both the monolayer state and the structural characteristics of INS at the interface, which are strongly influenced by the subphase pH and salt content. Brewster angle microscopy (BAM) was applied to investigate the peptide aggregation pattern at the air–water interface in the presence of the studied lipid under any experimental condition investigated. The influence of the lipid on the INS behavior at the interface strongly depends on the subphase conditions.

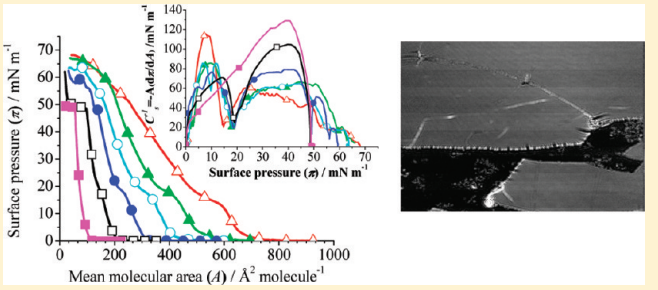

INTRODUCTION

Insulin[1] (INS) is a small protein[2] that is crucial for the control of glucose metabolism and in diabetes treatment. The active form of this hormone is the monomer, which is formed by two peptide chains: a hydrophilic chain called A, consisting of 30 amino acid residues, and another one called the B chain of hydrophobic nature with 21 amino acid residues. The two chains are covalently linked by two disulfide bridges.[3−5] The A chain forms two antiparallel α-helices, and the B chain forms an α-helix, turn, β-strand conformation.[6] This polypeptide hormone is synthesized and stored in the pancreas,[7,8] and the stored form is a Zn^{2+}-containing hexamer, which is composed of three equivalent dimers (6:2 INS/Zn^{2+}). These three structural forms, monomer–dimer–hexamer, exist in the bloodstream and in bulk solution in equilibrium; an equilibrium that depends on factors as INS concentration, pH, temperature, and so on.[9−13]

The number of people with diabetes has grown dramatically over the past decades, and it is estimated to increase in the next years.[14−17] Daily INS administration, by uncomfortable subcutaneous injections of the peptide (solutions or suspensions of Zn^{2+}-containing hexamers and synthetic forms) is required to achieve glycemic control of diabetic people, both type 1 and type 2. The parenteral route, despite its efficiency, implies many problems involving not only the intravenous injections but also the patient's quality of life.[18] During the past decades, many efforts have been made to find new INS dosage forms, which could alleviate these problems.[19−25] In this way, the first inhaled INS, approved in 2006, was used for the treatment of adult patients with type 1 (in association with longer-acting INS) and type 2 diabetes;[26,27] however, the manufacturer has voluntarily withdrawn the marketing authorization for the medicine in 2008.[28,29] Nowadays, more convenient alternative administration routes of INS, such as oral routes, are prevented because of the INS reduction to fragments by the peptidases of the gastrointestinal tract, even single amino acid components. In fact, only <1% of orally administered INS is absorbed.[30,31] As a consequence, the discovering of alternative routes that could alleviate the burden of INS injections would offer a good perspective for the diabetic patient. Thus, sustained release from different formulations opens up new prospects, as far some of these systems can protect INS from degradation in the gastrointestinal tract.[24]

It is known that INS is one of the proteins which are prone to aggregation and fibrillation. Thus, the peptide bulk solutions present stability problems as a consequence of the solid fibers formed by the monomers and the dimers under low pH conditions.[32] This causes the loss of the hormone biological activity and is an obstacle in developing new long-term delivery formulations.

Whereas the mechanism of aggregation of INS still remains unclear, within the past years, several studies have pointed out that some substances and diverse experimental conditions can vary the morphologies of the INS aggregates and the aggregation rates.[33−37] Furthermore, it has been reported that INS aggregation is accelerated by denaturants, for example, urea, whereas sucrose decreases the aggregation rate and stabilized the solutions.[38−40] More recently, other studies suggest that the presence of different hydrophobic environments, for example, air–water or lipid–water interfaces, can modulate the formation of these INS aggregates.[2,34,35,41]

Received: April 11, 2011
Revised: June 15, 2011
Published: June 20, 2011

It is known that the behavior of a drug inside the organism, in this case INS, depends on both the intermolecular interactions between the drug and other components in the pharmaceutical formulation and on their interactions with cell membranes, which are all dominated by surface effects. In this way, the design of new delivery systems, including different lipid phases to (i) stabilize the peptide solutions and (ii) protect INS inside the organism from degradation in a long-term delivery, implies a thorough knowledge of the intermolecular interactions between the peptide and the lipids used in the design of new pharmaceutical forms. Moreover, these studies could shed light onto the interactions of proteins with lipid interfaces and biological membranes by using properly chosen models with a well-defined lipid composition and adequate surface pressures.

The Langmuir monolayer technique is one of the methods used for studying the molecular behavior and the intermolecular interactions at the air−water interface.[42] In this method, the compounds of interest are first spread onto a water surface to form a monomolecular layer (so-called Langmuir monolayer). If this floating monolayer is prepared with two (or more) compounds, then the interactions between them can be estimated by the thermodynamic analysis made on the basis of the recorded surface pressure (π)−area (A) isotherms. To apply this technique, the molecules need to have an amphiphilic structure, which enables them to form monomolecular layers on free water surface. It is worth pointing out here that mixed Langmuir monolayers composed of different lipids from biological membranes provide a highly informative approach for studying intermolecular interactions between membrane components and biomolecules (like enzymes, proteins, hormones, or drugs). Many authors have used these simple in vitro membrane models to study the interactions between different proteins and membranes.[43−45] Because both substances, that is, INS and phosphatidylcholine (PC) have been reported to be capable of Langmuir monolayer formation, the technique seems to be an appropriate method to investigate their behavior at the interface as well as the nature and strength of their intermolecular interactions. We have also employed a Brewster angle microscope (BAM) to visualize the pure and mixed INS−PC monolayers spread at the air−water interface.

EXPERIMENTAL SECTION

Bovine insulin (>90% pure, < 5% H_2O) and PC (99%, pure) were supplied by Sigma Chemicals (5.733 kDa). L-α-PC is from egg yolk, and its fatty acid is ∼33% 16:0 (palmitic), 13% 18:0 (stearic), 31% 18:1(oleic), and 15% 18:2, (linoleic), which would give an average molecular weight of 768 g mol^{-1}. Both compounds were used as received and stored below 273 K. Spreading solutions of INS, with a concentration of ca. 0.6 mg mL^{-1}, were prepared in 0.06 M HCl (37% aq solution, Merck), whereas PC was dissolved in spectroscopic grade chloroform (Merck). Aqueous subphases were prepared with ultrapure water (resistivity 18.2 MΩ cm) produced by a Nanopure (Infinity) water purification system coupled to a Milli-Q water apparatus. $ZnCl_2$ (98%, Merck) was added as required to vary ionic strength, and NaOH and phosphate buffer were used to change the subphase pH. Routine experiments were carried out with a KSV 5000 (Finland) film balance, total area = 0.093 m^2 (0.775 × 0.120 m), equipped with two computer-controlled symmetrical mobile barriers and placed on an antivibration table. Surface pressure was measured with the Wilhelmy plate (made of paper) with an accuracy of ±0.05 mN m^{-1}. Monolayers were compressed with a barrier

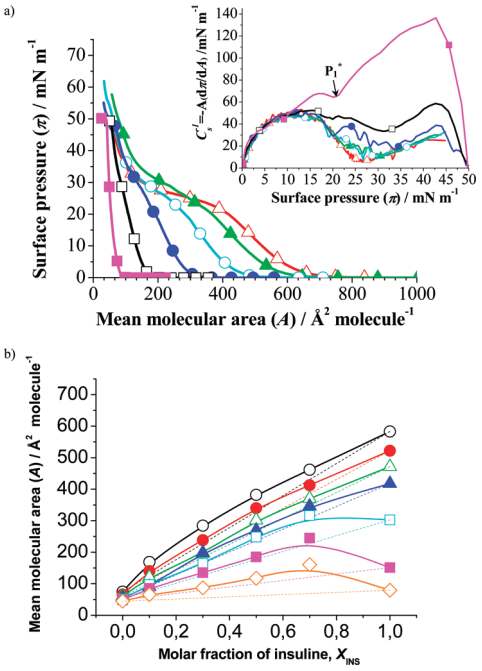

Figure 1. (a) Surface pressure−mean molecular area (π−A) compression isotherms for pure INS and PC monolayers and their mixtures spread on water subphase. Insert: Plots of compression moduli (C_s^{-1}) as a function of the surface pressure for pure and mixed monolayers. Insulin molar fraction: −△− (red), X_{INS} = 1; −▲− (green), X_{INS} = 0.7; −○− (light blue), X_{INS} = 0.5; −●− (dark blue), X_{INS} = 0.3; −□−(black), X_{INS} = 0.1; and −■− (pink), X_{INS} = 0. (b) Plots of A as a function of the insulin molar fractions at different surface pressures (−○−(black), 5 mN m^{-1}; −●− (red), 10 mN m^{-1}; −△− (green), 15 mN m^{-1}; −▲− (dark blue), 20 mN m^{-1}; −□−(light blue), 25 mN m^{-1}; −■− (pink), 30 mN m^{-1}; and −◇− (orange), 40 mN m^{-1}) for pure and mixed monolayers.

speed of 15 × 10^{-4} m s^{-1}. The subphase temperature (298 ± 1 K) was controlled thermostatically by a circulating water system. Langmuir monolayers were prepared by spreading an aliquot volume of the above-mentioned solutions. In the binary films, the PC solution was first introduced onto the air−water interface, and 10 min later the INS solution was dropped onto the whole surface. After spreading, the monolayers were left for 10 min; then, compression was initiated. All of the presented π−A isotherms have been selected after being reproduced in at least three independent experiments.

A Brewster angle microscope BAM 2 plus[46,47] (NFT, Germany) was used for microscopic observation of the INS−PC system. It is equipped with a 50 mW laser, emitting p-polarized light of 532 nm wavelength, which is reflected off the air−water interface at ∼53.15° (Brewster angle). The lateral resolution of the microscope was 2 μm. All equipment was placed on an antivibration table.

RESULTS AND DISCUSSION

Monolayers Spread on Water. Figure 1a shows the π−A isotherms recorded upon compression of pure monolayers of INS and PC and their mixtures of mole fractions (X_{INS}): 0.1, 0.3, 0.5, and 0.7. The behavior of pure INS monolayers spread at the air−water interface was already described in a previous paper.[48] The INS isotherm exhibits a plateau that starts at ∼25 mN m^{-1},

Table 1. Values of (a) Insulin Transition Pressure, π_t and (b) Monolayer Collapse Surface Pressure, π_c, for Both the Pure and Mixed INS-PC Monolayers Spread on Different Subphases (mN m^{-1})

(a)	transition pressure, π_t[a]					
		X_{INS}				
subphase	1	0.7	0.5	0.3	0.1	0
water	25.1	28.0	28.3	30.5	31.7	
NaOH pH 7.4	27.2	28.1	27.6	27.3	30.2	
phosphate buffer pH 7.4	23.0	23.1	24.2	25.0	25.4	
$ZnCl_2$						

(b)	collapse pressure, π_c[a]					
		X_{INS}				
subphase	1	0.7	0.5	0.3	0.1	0
water				51.1	50.3	50.4
NaOH pH 7.4	64.1	57.9	54.7	54.2	53.7	53.2
phosphate buffer pH 7.4				48.8	48.8	48.9
$ZnCl_2$	68.1	66.8	63.5	50.3	50.1	49.6

[a] Where possible.

the surface pressure at the beginning of the INS transition (π_t), and it was attributed to the hydrophobic B tails folding toward the air and the hydrophilic chain A partial immersing in the aqueous subphase upon compression. This occurs only when the peptide exists as monomer unfolded or partially unfolded at the interface.[48] PC isotherm corresponds to a condensed monolayer, which exhibits a liquid expanded (LE)−liquid condensed (LC) phase transition (~22 mN m^{-1}; P_1* in the insert of the Figure 1a), a value for the extrapolated area of the LC state to $\pi = 0$ (A_o) of 96 Å^2 molecule^{-1}, and a collapse pressure (π_c) of 50.4 mN m^{-1}. The compression isotherms recorded for mixed monolayers shift to lower areas at surface pressures below π_t as INS proportion decreases at the interface, and all of them exhibit the characteristic peptide transition described above. However, the length of this plateau drastically diminishes as the proportion of INS decreases in the monolayer, and the surface pressure increases upon compression, within this transition, in the presence of the lipid.

The surface compression modulus[49] [$C_s^{-1} = -A(d\pi/dA)$] versus surface pressure ($C_s^{-1}-\pi$) dependence (insert of Figure 1a) shows that both the pure INS monolayer and its mixtures are in a LE phase with values of C_s^{-1} lower than 60 mN m^{-1}, whereas values higher than 100 mN m^{-1}, which corresponds to a LC surface phase, were obtained only for the pure PC monolayer. Thus, the addition of INS to the PC film has a fluidizing effect evidenced by a drastic decreasing of C_s^{-1} for all mixtures at high surface pressures. The π_t value appears reflected as a minimum in the $C_s^{-1}-\pi$ curves at 25.1 mN m^{-1} for the pure INS film and for the mixture of X_{INS} = 0.7; however, π_t progressively increases while increasing the lipid molar fraction (X_{PC}) for mixed monolayers of $X_{INS} < 0.7$ to reach the value of ~31.7 mN m^{-1} for $X_{INS} = 0.1$. (See Table 1a.) The value of P_1*, ~21 mN m^{-1} in the pure PC monolayer, appears at the same surface pressure only in the mixtures of $X_{INS} < 0.5$. To examine the miscibility of the two film forming components, the analysis

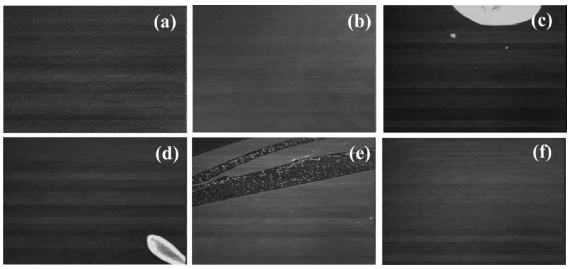

Figure 2. BAM images of PC and mixed INS/PC monolayers spread on water: (a) pure PC monolayer, $\pi = 0.1$ mN m^{-1}; (b) pure PC monolayer within the monolayer collapse, $X_{INS} = 0.1$; (c) within the monolayer collapse, $X_{INS} = 0.3$; (d) within the monolayer collapse, $X_{INS} = 0.5$; (e) within the monolayer collapse, $X_{INS} = 0.7$; and (f) within the monolayer collapse.

of the surface pressures values at which PC (P_1*) and INS (π_t) transitions start and monolayers collapse (π_c) can be helpful. Therefore, the variation of the transitions pressure and π_c with the molar ratio of the monolayer components could indicate their 2D miscibility.[50] Our results show that π_t increases with PC molar ratio when $X_{INS} < 0.7$; however, the values of P_1* and π_c, which only could be obtained for $X_{INS} < 0.5$, practically do not vary with the system composition. (See Table 1b.) On the basis of these results, we can only assume that INS and PC mix at the interface in monolayers of $X_{INS} < 0.7$ and at surface pressures below the INS transition.

The above conclusion was drawn solely upon analyzing the values of transitions and collapse surface pressures. Additional information to investigate the properties of the binary monolayers is obtained from the analysis of the variation of the mean molecular area as a function of the film composition. Figure 1b presents the $A-X_{INS}$ plots at several surface pressures corresponding to different surface monolayer states. From a thermodynamic approach, if the two components are immiscible or ideally miscible, the dependence of A versus X_{INS} should be linear because it results from the additively of the molecular areas. (It is shown by the dotted lines in Figure 1b.) Deviations from linearity indicate miscibility and nonideal behavior. Our system shows positive deviations, and the strength of these deviations depends on the monolayer composition and on the surface pressure. Therefore, at surface pressures lower than π_t, the excess area values increase as X_{INS} decreases, and once the peptide transition was started, they become higher and drastically increase as X_{INS} increases.

However, the sign and value of the excess area values alone are not decisive parameters regarding the miscibility between the film-forming components, but only its analyses together with the microscopic visualization of the monolayer morphology provide the complete characteristics of the 2D system at the interface. In this way, BAM has been applied for visualization of the investigated monolayers. The image in the Figure 2 shows the characteristic structures of the gas−LE phase transition for the pure PC monolayer; at surface pressures >0.2 mN m^{-1}, the film was homogeneous even within the collapse. (See image b.) The images obtained for pure INS and INS−PC mixtures spread on water have shown homogeneous films (images similar to image b and not shown) except within the monolayer collapse at surface pressures >50 mN m^{-1} (Figure 2c−e), where aggregates of PC can be observed at the interface, which drastically decrease in extension as the X_{INS} increases. For the X_{INS} = 0.7, a

dx.doi.org/10.1021/jp2033627 |J. Phys. Chem. B 2011, 115, 9387–9394

homogeneous film can be visualized even at the highest surface pressure reached upon film compression (image f).

Then, BAM images have demonstrated that the presence of PC at the interface does not provoke the aggregation of INS in the mixed monolayers spread on the air−water surface even within the monolayer collapse.

These results support the hypothesis of the two film-forming components being miscible until reaching the collapse and for any monolayer composition. Then, positive deviations from ideal behavior could be due to: (i) repulsive interactions between both components or (ii) less attractive forces in the binary monolayer than in the pure films. Therefore, considering the nature of the investigated molecules and bearing in mind that neither INS molecules (mainly dimers)[48] nor PC are net charged at pH 5.7, it does not seem that the increasing of area observed in the mixed monolayers, with respect to the pure films, could be a consequence of repulsive electrostatic interactions between INS and PC. In consequence, these positive deviations can be interpreted if we assume that the presence of the lipid at the interface affects the INS behavior by modifying the equilibrium ratio monomers ↔ dimers in the monolayer; furthermore, PC molecules partially avoid the unfolding of the INS monomers on the surface. Therefore, if the proportion of dimers increases with respect to monomers and the monomer's random structure is preserved in the monolayer by the intermolecular interactions established with the lipid molecules, then a higher proportion of INS residues remain on the surface once the peptide transition was started because the partial immersion of the chain A in the subphase should be partially prevented. This hypothesis is supported by: (i) the increasing of the positive deviations from ideality when INS transition was started and, furthermore, they become higher as X_{INS} increases, (ii) the drastic shortness of the plateau upon decreasing X_{INS}, and (iii) the progressive increasing of surface pressure upon compression (C_s^{-1}) in the mixtures within the peptide transition. At surface pressures lower than π_t, the excess area values decrease with respect to those described above for higher pressures, and they become higher as X_{INS} decreases. This fact could be caused by an increasing of the PC−PC intermolecular distance in the mixed monolayer due to the presence of the peptide at the interface; thus, hydrophobic intermolecular interactions in the mixed films are weaker than those established between the PC chains in the pure lipid monolayer.

Influence of the Subphase pH on the Behavior of the Monolayers. Figure 3a shows the isotherms obtained for the pure INS and PC monolayers and for their mixtures spread on a NaOH aqueous solution of pH 7.4. The main differences between the behavior of INS spread on water and on NaOH solution occur after starting the transition: (i) the isotherm is shifted to higher areas, (ii) the monolayer collapse pressure is reached at about 64.1 mN m^{-1}, and (iii) the characteristic INS plateau is shorter and, within this region, the surface pressure increases while A decreases. These results were interpreted assuming that the stability of the dimers is favored at pH 7.4; then, the dimer/monomer proportion becomes higher at the interface with respect to the monolayer spread on water.[48]

All mixed monolayers show the INS transition and π_t (~27 mN m^{-1}) does not vary with the film composition, except for the monolayer of X_{INS} = 0.1, where it increases ~3 mN m^{-1} (see Table 1a). The values of π_c showed in Table 1b vary with the monolayer composition for $X_{INS} > 0.5$, whereas for $X_{INS} \leq 0.5$, the films collapse at surface pressures similar to that recorded

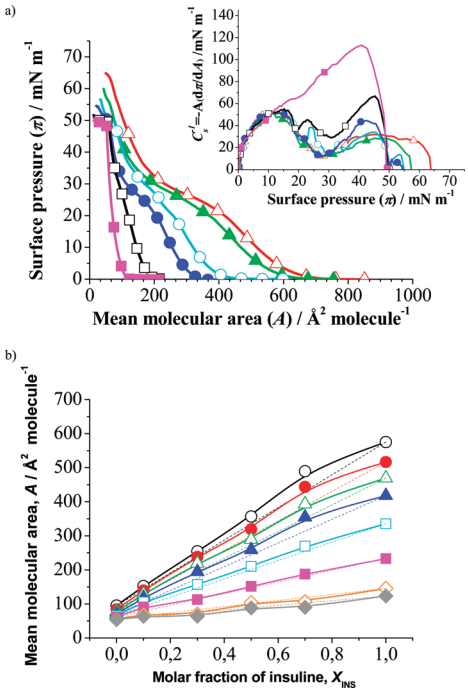

Figure 3. (a) Surface pressure-mean molecular area (π−A) compression isotherms for pure INS and PC monolayers and their mixtures spread on NaOH pH 7.4 subphase (ionic strength = 3.16 × 10^{-7} M). Insert: Plots of compression moduli (C_s^{-1}) as a function of the surface pressure for pure and mixed monolayers. Insulin molar fraction: (−△− (red), X_{INS} = 1; −▲− (green), X_{INS} = 0.7; −○− (light blue), X_{INS} = 0.5; −●− (dark blue), X_{INS} = 0.3; −□−(black), X_{INS} = 0.1; and −■− (pink), X_{INS} = 0. (b) Plots of A as a function of the insulin molar fractions at different surface pressures for pure and mixed monolayers. Plots of A as a function of the insulin molar fractions at different surface pressures (−○−(black), 5 mN m^{-1}; −●− (red), 10 mN m^{-1}; −△− (green), 15 mN m^{-1}; −▲− (dark blue), 20 mN m^{-1}; −□− (light blue), 25 mN m^{-1}; −■− (pink), 30 mN m^{-1}; −◇− (orange), 40 mN m^{-1}; −◆− (gray), 45 mN m^{-1}) for pure and mixed monolayers.

for the pure PC monolayer. Therefore, on the basis of the analysis of the dependence of π_t and π_c with the system composition, we can affirm only that the film-forming components are miscible in monolayers of $X_{INS} > 0.5$ at any surface pressure below π_c and in films of X_{INS} = 0.1 before reaching the INS transition. Furthermore, C_s^{-1}−π curves exhibit the characteristic minimum of the lipid LE−LC phase transition (P_1*) at ~20 mN m^{-1} for films of $X_{INS} < 0.7$.

Plots of mean molecular area versus surface pressure (Figure 3b) also show positive deviations from the ideality at surface pressures lower than 25 mN m^{-1}, and they are smaller than those previously described for monolayers spread on water. At higher surface pressures, the excess area values drastically decrease, and the dependence of A versus X_{INS} becomes near linear for any monolayer molar ratio. These results do not report information that could help to elucidate if the two film-forming molecules are miscible at surface pressures higher than π_t, as far as the additively rule is followed. Therefore, BAM images were taken for the pure and for the binary monolayers spread on NaOH solutions (see Figure 5). Pure INS film exhibits a homogeneous image within the whole compression (results not shown). However, characteristic structures of gas and LE phases can be observed for pure PC monolayers (image a), and

dx.doi.org/10.1021/jp2033627 |J. Phys. Chem. B 2011, 115, 9387–9394

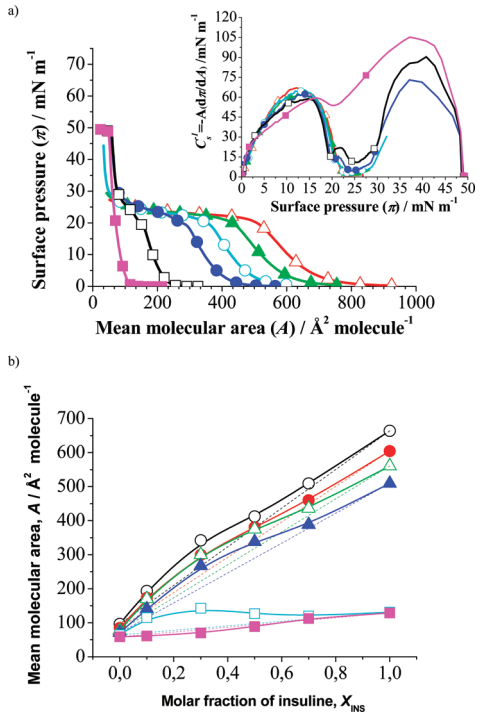

Figure 4. (a) Surface pressure−mean molecular area (π−A) compression isotherms for pure INS and PC monolayers and their mixtures spread on phosphate buffer pH 7.4 subphase (ionic strength = 0.193 M). Insert: Plots of compression moduli (C_s^{-1}) as a function of the surface pressure for pure and mixed monolayers. Insulin molar fraction: −△− (red), X_{INS} = 1; −▲− (green), X_{INS} = 0.7; −○− (light blue), X_{INS} = 0.5; −●− (dark blue), X_{INS} = 0.3; −□−(black), X_{INS} = 0.1; and −■− (pink), X_{INS} = 0. (b) Plots of A as a function of the insulin molar fractions at different surface pressures (−○−(black), 5 mN m^{-1}; −●− (red), 10 mN m^{-1}; −△− (green), 15 mN m^{-1}; −▲− (dark blue), 20 mN m^{-1}; −□− (light blue), 23 mN m^{-1}; −■− (pink), 27 mN m^{-1}) for pure and mixed monolayers.

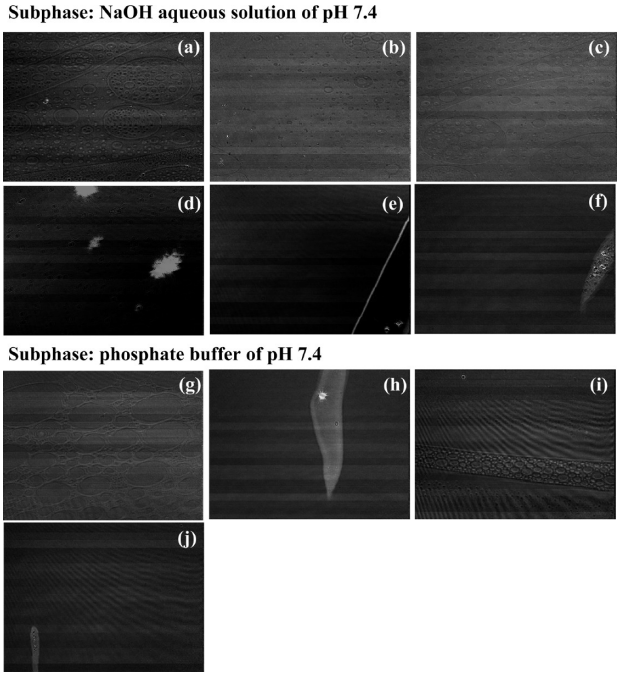

Figure 5. BAM images of PC and mixed INS/PC monolayers spread under different subphase pH conditions: on NaOH solution of pH 7.4: (a) PC, π = 0.5 mN m^{-1}; (b) X_{INS} = 0.1, π = 15.5 mN m^{-1}; (c) X_{INS} = 0.3, π = 17.3 mN m^{-1}; (d) X_{INS} = 0.3, π = 25.1 mN m^{-1}; (e) X_{INS} = 0.5, π = 29.4 mN m^{-1}; and (f) X_{INS} = 0.7, π = 48.7 mN m^{-1} and on phosphate buffer of pH 7.4: (g) PC, π = 0.1 mN m; (h) INS at the end of the transition; (i) X_{INS} = 0.1, π = 0.6 mN m^{-1}; and (j) X_{INS} = 0.7, π = 19.8 mN m^{-1}.

these structures can be only observed in the INS−PC mixed films of $X_{INS} \leq 0.3$ (images b and c); however, for higher INS molar fractions, they cannot be visualized. For X_{INS} = 0.3 and 0.5, 3D aggregates appear within the peptide transition (images d and e). However, for X_{INS} = 0.7, a homogeneous film was observed even at surface pressures higher than π_t, and some dispersed solid structures are only visible within the monolayer collapse (image f).

The above-described results prove that INS and PC mix only within the whole monolayer compression when X_{INS} = 0.7. However, for INS molar ratios of 0.5 and 0.3, the two monolayer components mix at surface pressures lower than π_t, but once the peptide transition was started they separate, and disperse 3D INS aggregates appear at the interface. These results prove that the presence of PC molecules in the monolayer spread on NaOH solution only induces the peptide aggregation at surface pressures higher than 25 mN m^{-1}, when the monolayer components separate at the interface. Therefore, INS aggregation occurs at the edges between domains of lipid and regions of peptide, where the pure INS 2D phase is in touch with PC molecules.

Figure 4a shows the isotherms for pure monolayers and for their mixtures spread on phosphate buffer subphase of pH 7.4. The INS isotherm is shifted toward larger areas as compared with that obtained on NaOH subphase at the same pH value. This is caused by the monolayer interaction with the subphase phosphate ions, which decreases the dimer/monomer proportion in the monolayer and favors the unfolding of the INS monomer chains at the interface.[48] Then, upon monolayer compression, INS and binary INS−PC monolayers exhibit the characteristic peptide plateau within larger range of areas than the films spread on NaOH solutions and on water.

The transition and collapse pressures do not vary with the film composition (see Table 1a,b). However, C_s^{-1} increases within the peptide transition for $X_{INS} \leq 0.3$, and the dependence of A versus X_{INS} (Figure 4b) shows positive deviations from ideality for $X_{INS} \leq 0.5$ at surface pressures lower than π_t, with a maximum for the X_{INS} = 0.3. Furthermore, the highest values of these deviations were obtained at 23 mN m^{-1}, just before starting the INS transition in the mixtures. However, films of $X_{INS} \leq 0.3$ exhibit opposite behavior of the excess areas at the end of the plateau (27 mN m^{-1}), where slight negative deviations can be observed. The positive deviations from ideality can be interpreted assuming a mixture at the interface where interactions between the film forming components are weaker than those in pure monolayers. INS is negatively charged in the presence of the subphase phosphate ions (−2 at pH 7.4)[51] and quasi fully extended at the interface. Therefore, the above-described positive deviations can be attributed to the existence of electrostatic interactions between the peptide and the lipid polar head. As a consequence, the PC polar head and the charged chain A delay its immersion into the subphase, and it causes an increase in the area per molecule at the interface. However, upon increasing π above π_t, the more soluble peptide chain starts to sink into the subphase; simultaneously, it provokes the

dx.doi.org/10.1021/jp2033627 |J. Phys. Chem. B 2011, 115, 9387–9394

reorientation of the ammonium group of PC toward the subphase at about 20−22 mN m^{-1}. Such a change strengthens the attractive electrostatic interactions in the partially submerged monolayer between the PC ammonium group and the negative-charged chain A. Therefore, the increasing of the C_s^{-1} values within the transition in mixed films of $X_{INS} \leq 0.3$ (with respect to the result obtained on NaOH) confirms the hypothesis of a more dense molecular packing state favored by the electrostatic interactions between INS and PC at $\pi > \pi_t$.

BAM images of pure and binary monolayers spread on buffered subphase are shown in Figure 5. Pure PC monolayer shows characteristic structures of gas phase at subphase pressures close to zero (image g) and, again, they can be observed only for $X_{INS} \leq 0.3$. INS monolayer has shown a homogeneous image until the end of the transition, where regions of high density and thickness with disperse 3D nuclei appear (image h). The images taken for binary monolayers exhibit these dense INS domains only for $X_{INS} = 0.7$ (image j). Then, BAM images support the hypothesis established on the thermodynamic results and demonstrate that: (i) INS does not aggregate in the mixed monolayers and (ii) the two film-forming molecules mix at the interface for $X_{INS} < 0.7$.

Influence of the Zn^{2+} Ions Dissolved in the Subphase on the Behavior of the Monolayers. To study the influence of Zn^{2+} ions on the behavior of INS/PC mixtures, an aqueous solution of $ZnCl_2$ of the ionic strength 0.015 M was used as subphase. In the absence of Zn^{2+} ions, the predominant structures of INS in bulk phases of pH 2−8 are dimers; therefore, under these conditions, the protein maintains its ternary structure at 298 K.[2,33,34] However, it is well known that these divalent cations can be incorporated into dimers, and it induces their association to form hexamers containing mainly three cations in their structure.[2,33,34] It has been previously described that upon spreading the peptide on an aqueous $ZnCl_2$ solution hexamers are also formed at the interface and they are stable under monolayer compression.[48] Because of this fact, both mixed and pure INS isotherms (Figure 6a) (i) do not exhibit the characteristic plateau originated for the submerging of the A chain into the subphase, (ii) the collapse pressures becomes higher and they can be measured for all the mixtures, and (iii) at high surface pressures A values drastically increase. Furthermore, values of C_s^{-1} (insert of Figure 6a) are higher than those obtained in the absence of Zn^{2+}. These results prove the condensing effect of the Zn^{2+} ions on the pure and mixed INS monolayers, which is caused by an increasing of the proportion of hexamers and dimers, with respect to monomers, at the interface.

The INS $C_s^{-1}-\pi$ curve exhibits a transition as a minimum at ∼15 mN m^{-1}, denoted by P^*_2 in the insert of Figure 6a, which is attributed to a change of orientation of the hexamers in the monolayer as a consequence of the pressure rise.[48] The value of P^*_2 increases as the proportion of PC increases in the monolayers until reaching a value of 19.3 mN m^{-1} for the film of $X_{INS} = 0.1$, and the monolayer collapse pressure decreases between the pure INS and the pure PC values (see Table 1b). On the basis of P^*_2 and π_c dependence with the monolayer composition, it may be concluded that INS oligomers and PC molecules should be miscible at the interface.

The dependence of A versus film composition (Figure 6b) exhibits slight positive deviations from ideality for $X_{INS} \leq 0.5$ at surface pressures lower than 15 mN m^{-1}; however, these deviations were observed for any monolayer composition at 17 mN m^{-1}. Upon increasing surface pressure, the system

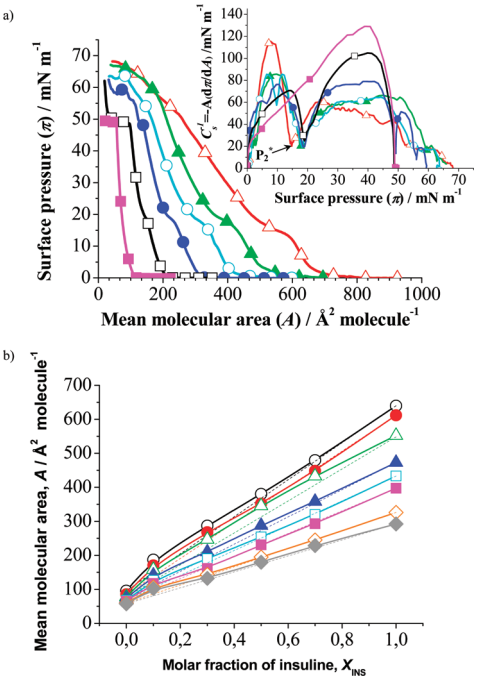

Figure 6. (a) Surface pressure−mean molecular area ($\pi-A$) compression isotherms for pure INS and PC monolayers and their mixtures spread on $ZnCl_2$ subphase (ionic strength = 0.015 M, pH 5.89). Insert: Plots of compression moduli (C_s^{-1}) as a function of the surface pressure for pure and mixed monolayers. Insulin molar fraction: −△− (red), $X_{INS} = 1$; −▲− (green), $X_{INS} = 0.7$; −○− (light blue), $X_{INS} = 0.5$; −●− (dark blue), $X_{INS} = 0.3$; −□−(black), $X_{INS} = 0.1$; and −■− (pink), $X_{INS} = 0$. (b) Plots of A as a function of the insulin molar fractions at different surface pressures (−○−(black), 5 mN m^{-1}; −●− (red), 10 mN m^{-1}; −△− (green), 17 mN m^{-1}; −▲− (dark blue), 20 mN m^{-1}; −□− (light blue), 25 mN m^{-1}; −■− (pink), 30 mN m^{-1}; −◇− (orange), 40 mN m^{-1}; −◆− (gray), 45 mN m^{-1}) for pure and mixed monolayers.

approaches ideal behavior for the monolayers of $X_{INS} > 0.1$. It has been assured that the hexamers of INS undergo the orientation change upon film compression (it occurs at ∼15 mN m^{-1} in the pure INS monolayer) in the way that the polar regions of the oligomers undergo submersion into the subphase. In such a state, these ternary structures occupy less area at the interface, as proved by the values of A at the beginning (∼604 $Å^2$ $molecule^{-1}$) and the end (∼ 503 $Å^2$ $molecule^{-1}$) of P_2*. In the mixed films, this change in the hexamers orientation occurs at pressures higher than 15 mN m^{-1} (insert of Figure 6a). As a consequence, the mixed isotherms are expanded with respect to the pure INS one at surface pressures between 15 and 20 mN m^{-1}. Therefore, as the oligomers change their orientation at higher surface pressure in the presence of PC molecules, A increases in the mixed films and it causes the positive deviations from ideality just at π = 17 mN m^{-1}. Upon increasing surface pressure, positive deviations prevail only for $X_{INS} = 0.1$, and this excess of area can be attributed to the isoelectric effect that exerts INS on the vertical oriented lipid molecules with respect to the air−water interface.

BAM images taken from pure PC monolayer spread on Zn^{2+} solutions exhibit only gas-phase structures at surface pressures close to zero (Figure 7, image a) and, upon increasing surface pressure, they were homogeneous within the whole compression (results not shown). Microscopic visualization of the pure

dx.doi.org/10.1021/jp2033627 |J. Phys. Chem. B 2011, 115, 9387–9394

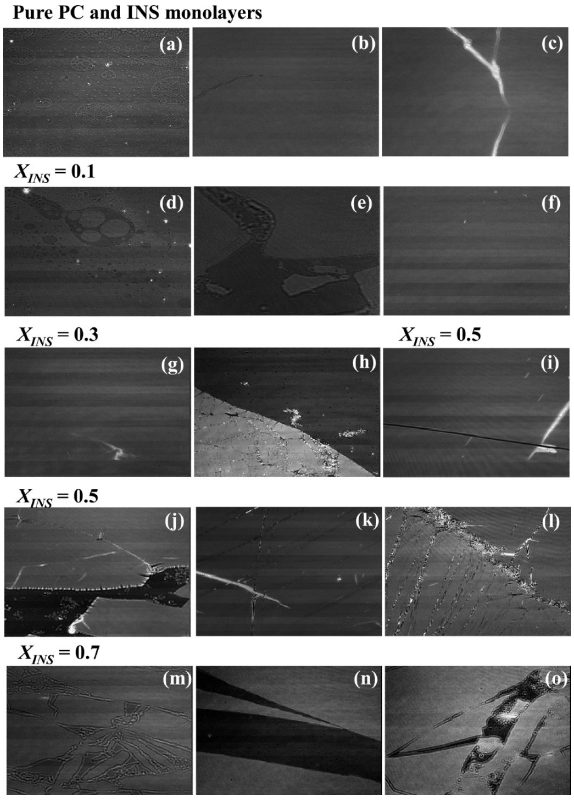

Figure 7. BAM images of pure and INS/PC mixed monolayers spread on $ZnCl_2$ I = 0.015 M subphase taken from different monolayer states and composition. Pure PC: (a) π = 0.5 mN m^{-1}. Pure INS: (b) π = 0.5 mN m^{-1}, and (c) collapse. X_{INS} = 0.1: (d) π = 0.1 mN m^{-1}, (e) π = 25.5 mN m^{-1}, and (f) π = 49.6 mN m^{-1}. X_{INS} = 0.3: (g) π = 45.3 mN m^{-1}, and (h) π = 57.8 mN m^{-1}. X_{INS} = 0.5: (i) π = 23.5 mN m^{-1}, (j) π = 32 mN m^{-1}, (k) π = 54.5 mN m^{-1}, and (l) π = 59 mN m^{-1}. X_{INS} = 0.7: (m) π = 4.7 mN m^{-1}, (n) π = 35.8 mN m^{-1}, and (o) π = 45.7 mN m^{-1}.

peptide monolayer shows homogeneous dense films (image b in Figure 7) until reaching the collapse, where INS starts to form long fibril aggregates at the monolayer edges and fractures (image c). In the binary monolayers, disperse 3D fibril structures appear at surface pressures of ~30 mN m^{-1} for X_{INS} of 0.3 and 0.5 (Figure 7g,j). As it can be clearly seen in the images, these aggregates start to form on the monolayer edges and fractures, as occurs in the pure peptide film, and they increase in number and length upon increasing surface pressure (Figure 7h,i,k,l). However, films of X_{INS} = 0.7 and 0.1 exhibit different behavior. Therefore, the system with the lower INS molar ratio shows only a few disperse nuclei within the gas−LE transition, which disappear upon increasing pressure (image d). In monolayers of X_{INS} = 0.7, INS does not form 3D aggregates, but at pressures close to 5 mN m^{-1}, the two monolayer components separate at interface (image m). This fact again supports the hypothesis established on the thermodynamic results and demonstrate that: (i) interestingly, for X_{INS} of 0.3 and 0.5, the two film-forming molecules separate at the interface at surface pressures of ~30 mN m^{-1}; then, the peptide starts to aggregate in the edges and fractures of the INS monolayer domains; (ii) INS does not aggregate in the monolayers of X_{INS} 0.1 and 0.7; and (iii) the peptide and the PC molecules form a mixture only at the interface within the whole monolayer compression for the lowest INS molar ratio.

CONCLUSIONS

Our results prove that the behavior of INS in the presence of PC at the air−water interface depends on both (i) the monolayer composition and (ii) the subphase pH and salts content. In the pure peptide monolayers, 3D long fibrils could be observed only on Zn^{2+} containing subphases. An important finding is that the presence of the PC molecules at the interface affects the INS behavior; however, the influence of the lipid on the peptide behavior strongly depends on the subphase conditions.

Thus, PC modifies the equilibrium ratio monomer ↔ dimers in the mixed monolayer spread on water. The lipid increases the proportion of dimers and partially avoids the unfolding of the INS monomers on the surface.

On NaOH subphases of pH 7.4, INS and PC are only miscible at the interface within the whole monolayer compression when X_{INS} = 0.7. The presence of PC in the monolayer induces the peptide aggregation, but it occurs only when the monolayer components separate at the interface and once the INS transition has been started. INS aggregation occurs at the edges between pure lipid domains and peptide regions, where INS is in touch with PC molecules. However, the monolayers behavior at the same pH value on phosphate buffer shows that: (i) the two film-forming molecules mix at the interface and (ii) INS does not aggregate in the mixed monolayers.

On Zn^{2+}-containing subphases, the two film-forming molecules separate only at the interface for X_{INS} of 0.3 and 0.5 and at surface pressures of ~30 mN m^{-1}. Under such conditions, the peptide again starts to form 3D aggregates in the edges and fractures of the pure INS monolayer domains. In the presence of the divalent cations, the peptide and the PC molecules only mix at the interface within the whole monolayer compression for the lowest INS molar ratio.

AUTHOR INFORMATION

Corresponding Author

*Tel: +34988387095. Fax: +34988387001. E-mail: nvromeu@uvigo.es.

ACKNOWLEDGMENT

This work was supported by the grant from the Ministerio de Educación y Ciencia (Spain) Rf. CTQ2009-08676, and to Xunta de Galicia for of Rf. 09CSA017383PR and IN845B-2010/062.

REFERENCES

(1) Banting, F. G.; Best, C. H.; Collip, J. B.; Campbell, W. R.; Fletcher, A. A. *Can. Med. Assoc. J.* **1922**, *7*, 141–146.

(2) Kraineva, J.; Smirnovas, V.; Winter, R. *Langmuir* **2007**, *23*, 7118–7126.

(3) Hansen, J. F.; Brange, J. *Protein Eng.* **1987**, *1*, 250.

(4) Brange, J.; Ribel, U.; Hansen, J. F.; Dodson, G.; Hansen, M. T.; Havelund, S.; Melberg, S. G.; Norris, F.; Norris, K.; Snel, L.; Sørensen, A. R.; Voigt, H. O. *Nature* **1988**, *333*, 679–682.

(5) Gunning, J.; Blundell, T. *The Peptides. Analysis, Synthesis, Biology*; Academic: New York, 1981.

(6) Brange, J.; Langkjaer, L. *Pharm. Biotechnol.* **1997**, *10*, 343–409.

(7) Chien, Y. W. *Drug Dev. Ind. Pharm.* **1996**, *22*, 753–789.

(8) Grodsky, G. M.; Forsham, P. H. *Annu. Rev. Physiol.* **1966**, *28*, 347–380.

(9) Adams, M. J.; Blundell, T. L.; Dodson, E. J.; Dodson, G. G.; Vijayan, M.; Baker, E. N.; Harding, M. M.; Hodgkin, D. C.; Rimmer, B.; Sheat, S. *Nature* **1969**, *224*, 491–495.

(10) Brange, J.; Langkjaer, L. Insulin Formulation and Delivery. In *Protein Delivery: Physical Systems*; Sanders, L. M., Hendren, R. W., Eds.; Plenum Press: New York, 1997; pp 343−412.
(11) Derewenda, U.; Derewenda, Z.; Dodson, E. J.; Dodson, G. G.; Reynolds, C. D.; Smith, G. D.; Sparks, C.; Swenson, D. *Nature* **1989**, *338*, 594–596.
(12) Smith, G. D.; Swenson, D. C.; Dodson, E. J.; Dodson, G. G.; Reynolds, C. D. *Proc. Natl. Acad. Sci. U.S.A.* **1984**, *81*, 7093–7097.
(13) Yip, C. M.; DeFelippis, M. R.; Frank, B. H.; Brader, M. L.; Ward, M. D. *Biophys. J.* **1998**, *75*, 1172–1179.
(14) Zimmet, P.; Alberti, K. G.; Shaw, J. *Nature* **2001**, *414*, 782–787.
(15) Wild, S.; Roglic, G.; Green, A.; Sicree, R.; King, H. *Diabetes Care* **2004**, *27*, 1047–1053.
(16) International Diabetes Federation. http://www.idf.org. Accessed Nov 22, 2010.
(17) WHO−Diabetes. http://www.who.int/diabetes. Accessed Nov 22, 2010.
(18) *Martindale: Guía Completa de Consulta Farmacoterapéutica*, 35th ed.; Pharma Editores: Barcelona, Spain, 2008.
(19) Cernea, S.; Raz, I. *Drugs Today* **2006**, *42*, 405–424.
(20) Jerry, N.; Anitha, Y.; Sharma, C. P.; Sony, P. *Drug Delivery* **2001**, *8*, 19–23.
(21) Setter, S. M.; Levien, T. L.; Iltz, J. L.; Odegard, P. S.; Neumiller, J. J.; Baker, D. E.; Campbell, R. K. *Clin. Ther.* **2007**, *29*, 795–813.
(22) Shao, Z.; Li, Y.; Chermak, T.; Mitra, A. K. *Pharm. Res.* **1994**, *11*, 1174–1179.
(23) Li, Y. z.; Quan, Y. s.; Zang, L.; Jin, M. n.; Kamiyama, F.; Katsumi, H.; Yamamoto, A.; Tsutsumi, S. *Biol. Pharm. Bull.* **2008**, *31*, 1574–1579.
(24) Sadrzadeh, N.; Glembourtt, M. J.; Stevenson, C. L. *J. Pharm. Sci.* **2007**, *96*, 1925–1954.
(25) Owens, D. R.; Zinman, B.; Bolli, G. *Diabetic Med.* **2003**, *20*, 886–898.
(26) Owens, D. R.; Grimley, J.; Kirkpatrick, P. *Nat. Rev. Drug Discovery* **2006**, *5*, 371–372.
(27) Lenzer, J. *BMJ [Br. Med. J.]* **2006**, *332*, 321.
(28) Public Statement on Exubera (Insulin Human) Withdrawal of the Marketing Authorisation in the European Union; European Medicines Agency (EMA): London, 2008. http://www.emea.europa.eu/docs/en_GB/document_library/Public_statement/2009/11/WC500007361.pdf. Accessed Nov 16, 2008.
(29) Insulin Administration. *Diabetes Care* **2004**, *27*, S106−S107.
(30) Carino, G. P.; Mathiowitz, E. *Adv. Drug Delivery Rev.* **1999**, *35*, 249–257.
(31) Oral Insulin 1922−1992: the History of Continuous Ambition and Failure. In *Frontiers in Insulin Pharmacology*; Berger, M., Gries, F., Eds.; Plenum Press: Stuttgart, Germany, 1993; pp 144−148.
(32) Owens, D. R. *Nat. Rev. Drug Discovery* **2002**, *1*, 529–540.
(33) Dzwolak, W.; Ravindra, R.; Lendermann, J.; Winter, R. *Biochemistry* **2003**, *42*, 11347–11355.
(34) Grudzielanek, S.; Jansen, R.; Winter, R. *J. Mol. Biol.* **2005**, *351*, 879–894.
(35) Grudzielanek, S.; Smirnovas, V.; Winter, R. *J. Mol. Biol.* **2006**, *356*, 497–509.
(36) Jansen, R.; Grudzielanek, S.; Dzwolak, W.; Winter, R. *J. Mol. Biol.* **2004**, *338*, 203–206.
(37) Smirnovas, V.; Winter, R.; Funck, T.; Dzwolak, W. *Chem. Phys. Chem.* **2006**, *7*, 1046–1049.
(38) Nielsen, L.; Frokjaer, S.; Carpenter, J. F.; Brange, J. *J. Pharm. Sci.* **2001**, *90*, 29–37.
(39) Nielsen, L.; Khurana, R.; Coats, A.; Frokjaer, S.; Brange, J.; Vyas, S.; Uversky, V. N.; Fink, A. L. *Biochemistry* **2001**, *40*, 6036–6046.
(40) Nielsen, L.; Frokjaer, S.; Brange, J.; Uversky, V. N.; Fink, A. L. *Biochemistry* **2001**, *40*, 8397–8409.
(41) Grudzielanek, S.; Smirnovas, V.; Winter, R. *Chem. Phys. Lipids* **2007**, *149*, 28–39.
(42) Gaines, G. L. *Insoluble Monolayers at Liquid−Gas Interfaces*; Interscience: New York, 1966.
(43) Lopes, D. H.; Meister, A.; Gohlke, A.; Hauser, A.; Blume, A.; Winter, R. *Biophys. J.* **2007**, *93*, 3132–3141.
(44) Meier, M.; Blatter, X. L.; Seelig, A.; Seelig, J. *Biophys. J.* **2006**, *91*, 2943–2955.
(45) Pérez-López, S.; Vila-Romeu, N.; Alsina Esteller, M. A.; Espina, M.; Haro, I.; Mestres, C. *J. Phys. Chem. B* **2009**, *113*, 319–327.
(46) Hoenig, D.; Moebius, D. *J. Phys. Chem.* **1991**, *95*, 4590–4592.
(47) Henon, S.; Meunier, J. *Rev. Sci. Instrum.* **1991**, *62*, 936–939.
(48) Nieto-Suárez, M.; Vila-Romeu, N.; Prieto, I. *Thin Solid Films* **2008**, *516*, 8873–8879.
(49) Gaines, G. L. Properties of Liquid Surface. In *Insoluble Monolayers at Liquid−Gas Interfaces*; Prigogine, I., Ed.; Interscience: New York, 1966; p 24.
(50) Dynarowicz-Latka, P.; Kita, K. *Adv. Colloid Interface Sci.* **1999**, *79*, 1–17.
(51) Hong, D. P.; Ahmad, A.; Fink, A. L. *Biochemistry* **2006**, *45*, 9342–9353.